[12] Y. Nashimoto, S. Ichikawa, N. Samoto, K. Onda, M. Kuzuhara, and K. Arai, "Super-low noise heterojunction field-effect transistors (HJFETs) with 0.2-μm T-shaped 8 gate fingers," *NEC Res. Dev.*. vol. 33, pp. 268–272, July 1992.

Reflection-Type Low-Phase-Shift Attenuator

Won-tae Kang, Ik-soo Chang, and Min-soo Kang

***Abstract*— A transmission-type phase-shift attenuator has a poor reflection characteristic at an output port. In this paper, to avoid such disadvantages, a reflection-type low-phase-shift attenuator has been designed and measured. As a result, at a center frequency (1855 MHz), the reflection-type low-phase-shift attenuator has an attenuation of 30 dB, within the limit of 3° phase shift and less than −17-dB reflection characteristics at both input and output ports. It also demonstrates that the performance of the reflection-type low-phase-shift attenuator is better than the transmission-type phase-shift attenuator with the same measurement specifications.**

***Index Terms*—Attenuator, p-i-n diode, reflection type.**

I. Introduction

The circuits generally used in the transmitter of the base station of a modern mobile-communication system consist of high-power amplifiers, linearizers, and so on. The variable attenuator is especially one of the most important control circuit blocks composing linealizers, as well as automatic gain control (AGC) systems. Generally, the attenuators are implemented by using a p-i-n diode or GaAs MESFET with electrically controllable resistance [1] and, in this paper, p-i-n diodes are applied.

A radio-frequency (RF) signal is composed of both magnitude and phase elements, but the phase characteristics can be distorted with the variance of attenuation due to the following structural problem.

In Fig. 1, the S-parameters of the series impedance Z are given by [2]

$$[S] = \begin{bmatrix} \dfrac{Z}{Z+2Z_0} & \dfrac{2Z_0}{Z+2Z_0} \\ \dfrac{2Z_0}{Z+2Z_0} & \dfrac{Z}{Z+2Z_0} \end{bmatrix}. \tag{1}$$

The attenuation constant α can then be written as

$$\alpha = 20\log\left|\frac{1}{S_{21}}\right| = 20\log\left|1+\frac{R+jX}{2Z_o}\right| = 10\log\left[\left(1+\frac{R}{2Z_o}\right)^2+\left(\frac{X}{2Z_o}\right)^2\right]. \tag{2}$$

In the general case of attenuators, the phase characteristic of S_{21} is

$$S_{21} = |S_{21}|e^{\varphi} = \frac{2Z_o}{(Z+2Z_o)} \tag{3}$$

$$\rightarrow \varphi = \tan^{-1}\frac{-X}{R+2Z_o}. \tag{4}$$

Manuscript received March 27, 1997; revised April 7, 1998.

The authors are with the Department of Electronic Engineering, Graduate School of Sogang University, Seoul 100-611, Korea.

Publisher Item Identifier S 0018-9480(98)04944-8.

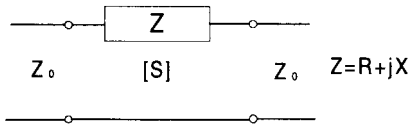

Fig. 1. The equivalent circuit of attenuator.

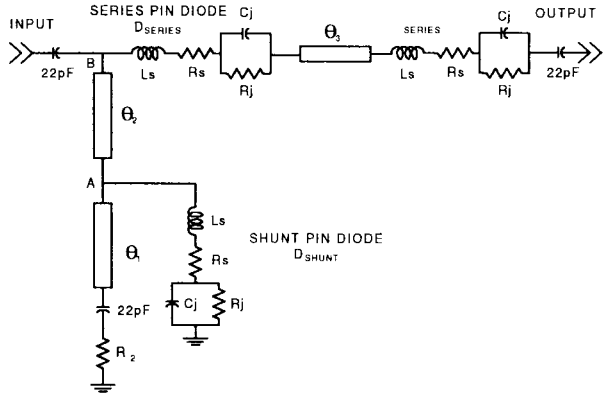

Fig. 2. Transmission-type low-phase-shift attenuator.

As we can observe in (4), the phase characteristic is variable with the variance of attenuation because φ is a function of R. To solve this kind of structural problem, Walker [3] invented the transmission-type attenuator using p-i-n diodes.

Fig. 2 shows the modified Walker version. It was invented in order to enlarge the attenuation by using series connected diodes.

In this circuit, series-connected p-i-n diodes operate as attenuators, while a shunt-connected diode operates as a phase-shift compensation circuit. The characteristic of intrinsic layer resistance of a p-i-n diode is given by [1]

$$R = \frac{W^2}{(2\mu_{ap}\tau I_0)} \tag{5}$$

where

- W width of i layer;
- μ_{ap} ambipolar mobility;
- τ carrier lifetime;
- I_0 dc bias current.

By forward biasing the diodes in Fig. 2, I_o is increased and R_j is near 0 Ω, as can be observed in (5). At this time, the attenuation is minimum and the R_j of the shunt-connected p-i-n diode goes to zero. Thus, point A turns out to be a short and the shunt-connected stub at point B will be sensed as the short stub with electrical length θ_2. For this reason, there is no attenuation caused by R_2.

Alternatively, if I_o is decreased by reverse biasing, then R_j is increased. Thus, the shunt-connected stub at point B has an effect on the entire circuits.

Let the phase of the total system be $\varphi_{R_j=0}$ at $R_j = 0$, and $\varphi_{R_j=\max}$ at $R_j = \max$. If it is possible that $\varphi_{R_j=0} = \varphi_{R_j=\max}$ with controlling θ_1, θ_2, θ_3, and R_j, then no phase shift occurs with the variance of attenuation.

The parameter values of $R_2 = 15\ \Omega$, $\theta_1 = 15°$, $\theta_2 = 16.46°$, and $\theta_3 = 14.28°$ are applied in experiments.

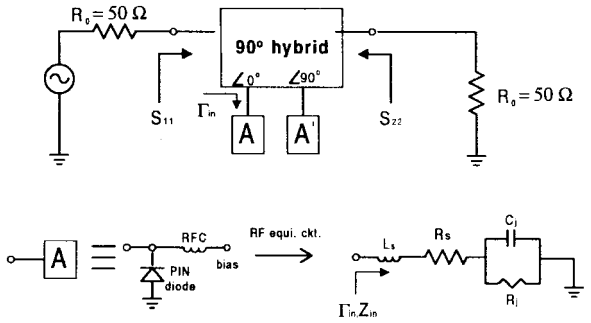

Fig. 3. Reflection-type attenuator.

II. Design of Reflection-Type Attenuator

The weak points of a transmission-type low-phase-shift attenuator are as follows. First, S_{22}, the reflection coefficient at the output port, is not good. Second, because it is a current-controlled attenuator, the attenuation decreases when output current is limited. Thus, the variation range of AGC will be decreased. To overcome this problem, the new reflection-type attenuator is proposed in this paper, as shown in Fig. 3.

Fig. 3 shows the attenuator using a reflection characteristic; thereby differing from the transmission-type attenuator used before, and because it uses a 90° hybrid, it has the same characteristics at both A and A', and gives a good matched condition in both S_{11} and S_{22} by symmetric structure.

The operation of the reflection-type attenuator can be explained as follows. In Fig. 3, in the case of $Z_{\rm in} = 50\ \Omega$, since the RF signal is all consumed at point A, it is not transmitted to the load at isolation port and, thus, the attenuation becomes maximum.

On the other hand, when $Z_{\rm in} = 0\ \Omega$ or $Z_{\rm in} = \max$, the RF signal is completely transmitted to the load because of the total reflection at port A. In this case, the attenuation is 0 dB.

At this condition, the phase characteristic of reflection-type attenuator is

$$\varphi = \angle\,\Gamma_{\rm in} = \tan^{-1}\left[\frac{wL_s - \dfrac{wR_j^2C_j}{1+w^2R_j^2C_j^2}}{R_s - Z_o + \dfrac{R_j}{1+w^2R_j^2C_j^2}}\right] - \tan^{-1}\left[\frac{wL_s - \dfrac{wR_j^2C_j}{1+w^2R_j^2C_j^2}}{R_s + Z_o + \dfrac{R_j}{1+w^2R_j^2C_j^2}}\right]. \quad (6)$$

As shown in (6), the phase characteristic varies with the variation of R_j. That can be explained as the effects of the parasitic elements C_j, L_s on a p-i-n diode. Thus, if these parasitic elements can be adequately compensated, the phase characteristic keeps constant for the variation of R_j.

It can be implemented as follows, using an open stub as the phase compensation circuit.

In this case, $Z_{O.c}$ is expressed as follows:

$$Z_{O.C} = Z_0\,\frac{Z_L + jZ_0\tan\theta}{Z_0 + jZ_L\tan\theta} \Leftarrow Z_L = \infty = \frac{Z_0}{j\tan\theta}. \quad (7)$$

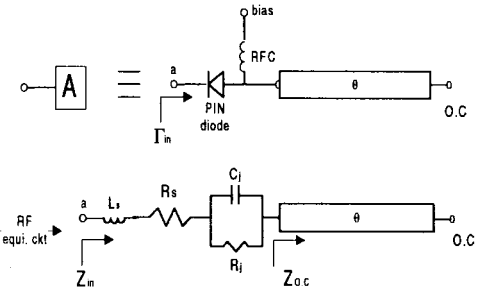

Fig. 4. The phase compensation circuit with an open stub.

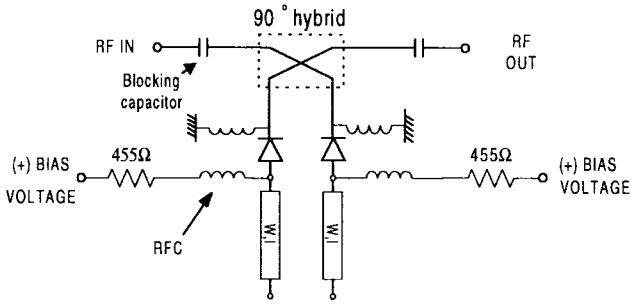

Fig. 5. Reflection-type low-phase-shift attenuator.

Therefore, we obtain $Z_{\rm in}$ by applying (7) to Fig. 4, resulting in

$$Z_{\rm in} = R_s + jwL_s + \frac{1}{\dfrac{1}{R_j} + jwC_j} + Z_{o.c} = R_s + \frac{R_j}{1+jwR_jC_j} + j\left(wL_s - \frac{Z_0}{\tan\theta}\right) \quad (8)$$

because coefficient $\Gamma_{\rm in} = |\Gamma_{\rm in}|e^{\varphi} = (Z_{\rm in} - Z_o)/(Z_{\rm in} + Z_o)$, φ is given by

$$\varphi = \tan^{-1}\left[\frac{wL_s - \dfrac{wR_j^2C_j}{1+w^2R_j^2C_j^2} - \dfrac{Z_o}{\tan\theta}}{R_s - Z_o + \dfrac{R_j}{1+w^2R_j^2C_j^2}}\right] - \tan^{-1}\left[\frac{wL_s - \dfrac{wR_j^2C_j}{1+w^2R_j^2C_j^2} - \dfrac{Z_o}{\tan\theta}}{R_s + Z_o + \dfrac{R_j}{1+w^2R_j^2C_j^2}}\right]. \quad (9)$$

Let the phase of the total system at $R_j = 50\ \Omega$ be $\varphi_{R_j=50}$, and the phase of the total system at $R_j = \max$ be $\varphi_{R_j=\max}$. Since φ is a function of θ, we can implement a low-phase-shift attenuator if the condition of $\varphi_{R_j=0} = \varphi_{R_j=\max}$ is achieved by adjusting the θ value.

III. Experimental Results

Fig. 5 is the circuit of low-phase-shift attenuator using a p-i-n diode. In this paper, Hewlett-Packard's HSMP-4810 p-i-n diode is applied. The equivalent circuit of the diode is solved by the Deloach method [4], and the parameter values are $C_j = 0.2034$ pF, $L_s = 1.748$ nH, and $R_s = 3.342\ \Omega$.

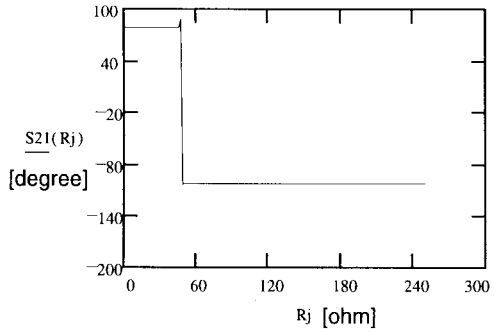

Fig. 6. The phase variance of S_{21} for R_j variance at the electrical length of open-stub is 73.1°.

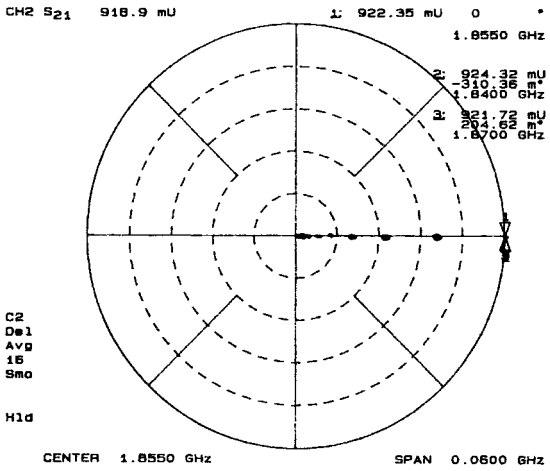

Fig. 7. The electrical characteristic of low-phase-shift attenuator.

By using these parameter values and MATHCAD computer software, 73.1° electrical length of the open stub is calculated, and the simulation result of this condition is shown in Fig. 6.

For this experiment, TLC-32 substrate, a Taconic product, with relative permittivity $\varepsilon_r = 3.2$ is used. The center frequency is 1855 MHz. In Fig. 5, the length of the open stub is 21.4 mm and its width is 1.85 mm. The 90° hybrid of the attenuator is the BJC2 type manufactured by SAGE products, having broad-band characteristics and a length of 19.5 mm.

The electrical characteristic of the low-phase-shift attenuator is shown in Fig. 7.

Figs. 8 and 9 show the measured results of comparison data of transmission and reflection type, which demonstrate the better performance of reflection type.

IV. Conclusion

In this paper, a reflection-type low-phase-shift attenuator is shown to overcome some disadvantages of the previous transmission-type phase-shift attenuator. The reflection-type low-phase-shift attenuator has been designed such that it has no more than 3° phase shift with up to 30-dB attenuation, and return loss below 17 dB at both input and output ports.

With the previous transmission-type phase-shift attenuator, used as an AGC component, the output current of the attenuation controller must be small and, thus, the dynamic range of the attenuator is small. Even so, the output-port reflection characteristic is not good, but the reflection-type low-phase-shift attenuator solves both the current

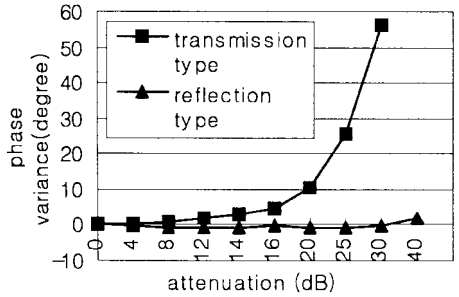

Fig. 8. The phase variance comparison of transmission and reflection type.

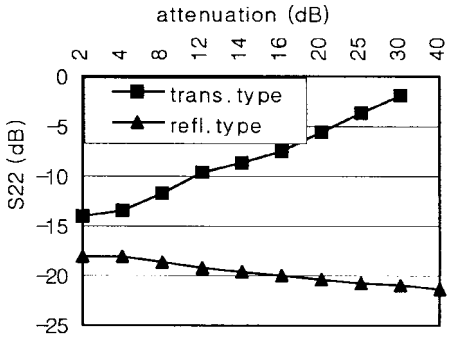

Fig. 9. The S_{22} comparison of transmission and reflection type.

limitation problem with a diode that operates at high resistance and the poor reflection characteristic problem at output port due to the 90° hybrid.

By using the MATHCAD program, 73.1° electrical length of the short stub was calculated, but experimentally, 76.34° was obtained—an error of approximately 3°. The error can be described as due to the simplified diode model employed by the diode parameters with the Deloach method, and of the same application of the diode parameters as under zero-bias without considering the variation of the diode parameters under forward-bias. To decrease the error, further study in evaluating the diode parameters is necessary.

References

[1] I. Bahl and P. Bhartia, *Microwave Solid State Circuit Design.* New York: Wiley, 1988, pp. 667–670.

[2] K. Chang, *Microwave Solid-State Circuits and Applications.* New York: Wiley, 1994, pp. 86–90.

[3] S. Walker, "A low phase shift attenuator," *IEEE Trans. Microwave Theory Tech.*, vol. 42, pp. 182–185, Feb. 1994.

[4] B. C. Deloach, "A new microwave measurement technique to characterize diodes and an 800-Gc cutoff frequency varactor at zero volts bias," *IEEE Trans. Microwave Theory Tech.*, vol. MTT-12, pp. 15–20, Jan. 1964.